Environmental Science and Pollution Research (2021) 28:57602–57618
https://doi.org/10.1007/s11356-021-14640-9

RESEARCH ARTICLE

A relative study on energy and exergy analysis between conventional single slope and novel stepped absorbable plate solar stills

Gurukarthik Babu Balachandran[1] · Prince Winston David[1] · Anandha Balaji Alexander[1] · Muthu Manokar Athikesavan[2] · Padmanaban Velayudha perumal Chellam[3] · Krishna Kumar Sasi Kumar[1] · Vinothkumar Palanichamy[1] · Abd Elnaby Kabeel[4] · Ravishankar Sathyamurthy[5] · Fausto Pedro Garcia Marquez[6]

Received: 3 March 2021 / Accepted: 26 May 2021 / Published online: 5 June 2021

Abstract

The innovation of novel absorbing materials using composite materials and nanotechnology is of new trends for many researches. Here, the present study is concerning to enhance the distilled water productivity of a proposed solar still (PSS) using novel absorbing materials. The absorbing material is composed of chitosan (obtained from waste shrimp shells), ethylene diamine tetraacetic acid (EDTA), and *Chrysopogon zizaniodes* (Vetiver). The combination of these materials is coined as CHEDZ, and it acts as a super absorbent polymer that is coated on the stepped solar still. Evaporation rate increases due to this absorbent, which further increases the yield of the still. In this present study, the PSS is compared with the conventional solar still (CSS) for the use of assessing the yield of freshwater in the same atmospheric circumstance. The experimental setup was performed through the period from December to February 2020 in the Indian climatic condition. The freshwater productivity was improved to 3.05 L/day while the yield of the CSS is 2.47 L/day. The increase in efficiency obtained from a PSS is 39.71% more than the productivity attained from the CSS. The energy efficiency of the PSS is 18.34% and the exergy efficiency is 0.45%.

Keywords Stepped absorbable plate · CHEDZ · Super absorbent · Renewable energy

Highlights of this study:
- The present study is concerning to enhance the distilled water productivity of a proposed solar still (PSS) using novel absorbing materials.
- The absorbing material is composed of chitosan (obtained from waste shrimp shells), ethylene diamine tetraacetic acid (EDTA), and *Chrysopogon zizaniodes* (Vetiver). The combination of these materials is coined as CHEDZ, and it acts as a super absorbent polymer that is coated on the stepped solar still.
- The increase in efficiency obtained from a PSS is 39.71% more than the productivity attained from the CSS. The energy efficiency of the PSS is 18.34% and the exergy efficiency is 0.45%.

Responsible Editor: Philippe Garrigues

✉ Gurukarthik Babu Balachandran
mspsbguru@gmail.com

✉ Fausto Pedro Garcia Marquez
FaustoPedro.Garcia@uclm.es

[1] Department of Electrical and Electronics Engineering, Kamaraj College of Engineering and Technology, Madurai, Tamil Nadu 625 701, India

[2] Department of Mechanical Engineering, B.S. Abdur Rahman Crescent Institute of Science and Technology, Chennai 600 048, India

[3] Department of Bio Technology, Kamaraj College of Engineering and Technology, Madurai, Tamil Nadu 625 701, India

[4] Mechanical Power Engineering Department, Faculty of Engineering, Tanta University, Tanta, Egypt

[5] Department of Mechanical Engineering KPR Institute of Engineering and Technology, Arasur, Tamil Nadu Coimbatore, India

[6] Ingenium Research Group, Universidad Castilla-La Mancha, Ciudad Real, Spain

Introduction

There is a need for freshwater in many countries. Most of water cannot be used for drinking purposes (Essa et al. 2020; Parsa et al. 2020; Yousef and Hassan 2020). The water paucity is a serious problem in the world (Sharshir et al. 2020b; Sharshir et al. 2020a; Elashmawy 2020). The world population would increase, and the water paucity also increases. There are many techniques used for water desalination. But solar still desalination is an ancient method, and many modifications have been incorporated to enhance the productivity of the still (Kabeel et al. 2019; Kabeel et al. 2020; Thalib et al. 2020; Sathyamurthy et al. 2020).

Experimental analysis of the conventional solar still (CSS) with pin finned wick was studied by Alaian et al. (2016). These materials are supported on the basin surface of the CSS by adopting aluminum steel lines. By adopting pin finned wick in the CSS, efficiency of the still was improved to 55%, and the productivity of the CSS was nearly 23%. Arunkumar et al. (2018) investigated the CSS with various types of insulation: One with carbon impregnated foam with bubble wall insulation; other with wooden insulation; and the third one with bubble wall insulation. They were compared with CSS. From this, carbon impregnated foam with bubble wall insulation enhanced the productivity to 3.1 L/m^2. Rabhi et al. (2017) used pin finned wick and an external condenser to improve the still output. 32.18% gain in the production was observed when the condenser was connected externally to the CSS.

Balachandran et al. (2020c) reported the enhancement of a CSS by using water film cooling and hybrid composite insulation. The hybrid natural fiber composite insulation consists of nano-silica, e.g., Pharsalus Vulgaris along with instated polyester wax. In addition to the film, cooling was also done over the glass surface leading to an increase in productivity, and the daily yield obtained was 1.420 L/day. Experimental analysis on CSS using various wick components was published by Bhargva and Yadav (2019). Various wick materials like bamboo cotton, jute, and wool were used to increase the productivity. The wick materials are dyed black to increase the absorption rate and are placed inside the rectangular fins arrangement. From the various wick materials, bamboo cotton increases the productivity rate to 3.03 L/m^2/day, and the efficiency was around 34.5%, which is more than the jute and cotton. Chen et al. (2019) experimentally investigated a study on the application of recoverable carbon nanotube used for solar water desalination. They used magnetic multi-walled carbon nanotubes obtained using Fe_3O_4. By using this material, heat transfer rate increases, which increases the yield of the still. The still incorporated with multi-walled carbon nanotubes increases the efficiency to 24.91%, which is higher than the CSS. Chen et al. (2018) designed the electrospun nanofiber membrane prepared by using magnesium aluminum-ethylene diamine tetraacetic acid-lactate dehydrogenase (MgAl-EDTA-LDH) for investigating the absorption properties of copper from the waste water. They prepared a new adsorbent which was synthesized by EDTA into double-layered hydroxides. Therefore, the waste water gets treated by using the copper, and the absorption capacity was around 120.77 mg/g. An empirical investigation on modification the performance of single slope double basin solar still was studied by Gnanaraj and Velmurugan (2019). They have experimentally conducted an investigation on three stills (still with finned corrugated basin, black granite, and external reflectors). Black granite combined with external reflectors enhanced the yield to 5.13 L/m^2 compared to the CSS, which is 1.88 L/m^2. The finned corrugated basin on double basin still increases the efficiency to 58.47%. Haddad et al. (2017) improved the CSS performance by adopting a perpendicular rotary wick. A rotating black wick belt was combined across the black surface to increase the additional collector evaporator rate. By using this performance of the still improvements, the yield of the still was 5.03 kg/m^2, and the efficiency of the still was 51.1%.

Hansen et al. (2015) researched an inclined solar still with different new wick elements and wire mesh. Various wick elements related to the wood pulp, coral fleece, and polystyrene sponge were recycled in flat absorbable and stepped absorbable plates. The maximum yield of 4.28 L/day was reported when adopting coral fleece along with wire mesh coated on the stepped type absorbable plate. Harish Prashanth and Tharanathan (2006) studied the preparation and characterization of cross-linked chitosan. They used shrimp shells, and it was demineralized using HCl and then deproteinized using the NaOH solution. The obtained powder was treated with an acetic acid solution to obtain chitosan powder. Design parameters on still using phase changing materials were studied by Khandagre et al. (2019). The experimental investigation was done on a double slope still. The basin was coated by using a blackened absorbing surface, and the phase changing material (PCM) (paraffin wax) was placed on the still basin, which was called as an organic PCM. The comparison study was done between organic and inorganic PCM. Eutectics are used as an inorganic PCM. By using this yield of the still, it improves from 8.02 to 8.07 L/m^2/day, which was more than the CSS, whose improvement was 4.01 to 4.34 L/m^2/day. Performance augmentation of still using efficient heat exchange mechanism was experimentally done by Kabeel et al. (2017). They enhanced the still performance by using paraffin wax along with sodium chloride solution, and it is placed under the basin of the still. Due to this, the heat transfer rate increases and, at the same time, the cover cooling was done on the top surface of the still. The productivity obtained was 4.535 L/m^2, and the efficiency was around 36.2 %, which is higher than the CSS. Fath and Hosny (2002) studied a process to improve the CSS. The design modification compassed is using an inbuilt condenser to heat the water, and the insulation provided is by means of rock wool insulation to maintain the inner heat. The internal

mirrors were also used on the sides of the still to augment the evaporation amount. The distillate efficiency of the still is around 18–27% compared to an identical still without modifications. Kudret Selçuk (1964) designed and studied the multi-effect tilted solar still performance. In an active still, the feed water is taken through the pump, and the flat plate collector is used to preheat the input water through internal reflectors, and it is given to the still. Black wick insulation was coated on the basin of the still to increase the desalination rate. The still output was observed to be 4.2 L/day. The conduct of a single slope twin basin still along with a wick elements was published by Modi and Modi (2019). They used two wick materials like jute cloth and black cotton cloth with a small pile, and they were used as an absorbing material. The little pile of brunet cotton material exploits as a brunet absorbing expanse compared to jute material as a non-brunet absorbing expanse. Therefore, distillate output gets increased by using a black cotton cloth, and the efficiency was around 21.46%. Rahim (2001) used a horizontal aluminum plate above the basin of the still to receive the maximum amount of solar radiation, and it is used to heat the top surface of the water to improve productivity. The experiment was tested at a water depth of 2 m, and the efficiency was obtained to 28%.

Ni et al. (2018) reported the performance of the still by salt, rejecting floating solar still. The salt-deny structure frequently conducts under sunlight to obtain fresh vapor while floating on a briny water body. It was incorporated inside the still. The corrugated wick was placed inside the solar still with internal reflectors, integrated with an external condenser. The arrangement was coupled with a polymer covering to obtain distilled water. The efficiency percentage increases to 2.5 L/day. Pal et al. (2017) designed the modified basin type dual-slope wick still with black cotton wick was placed on the top surface of the still. The wick was hung on the wick rods on both sides of the double basin. By using a black cotton wick, the evaporation rate increases, and the distillate output increases. The yield of the still was around 4.50 L/m^2/day, and the efficiency of the still was 23.03%. Panchal and Mohan (2017) enhanced the distillate output of the double basin still using vacuum pipes. They used various energy storage materials, e.g., calcium stones, black granite gravel, and pebbles on the basin surface of still. The calcium stone was considered as a heat-absorbing material next to its black granite gravel, considered as an absorbing material. The distillate productivity showed that basin surface with calcium stones were better compared with pebbles and black granite. The calcium stones incorporated with vacuum pipes increase the efficiency to 74%. Patel et al. (2019) designed the productivity enhancement of still by integrating evacuated tubes and obtaining potable water by solar thermal distillation. The experiment was done on stepped type absorbable plates. The feed water was taken through the evacuated tubes, and it was given as an input to the still. By the proposed methodology, the efficiency of the still gets enhanced, and the distillate yield increases. Therefore, using stepped still with an evacuated tube collector increases the efficiency to 24%, and the yield of the still was around 8.1 L/day. Suneesh et al. (2016) augmented distillate productivity in v-type tilted wick still using cotton gauze cooling under regenerative effect. The experiment was done on v-type still with fin-type, and the feed water was taken through the pump. It was given through the hot reservoir and fed to the tilt basin. The cotton gauze was used as an absorbing material that was placed on the fin-type basin, and the distillate yield of the still was around 6.3 L/m^2. Ritonga et al. (2019) have experimentally prepared chitosan EDTA hydrogel as a soil invigorator for a soybean plant. The result shown that hydrogel synthesized by chitosan and EDTA has been used as a smudge stimulant. Sabaa et al. (2015) experimentally studied the synthesis, characterization, and utilization of biodegradable cross-linked carboxymethyl chitosan nanoparticles. The nanoparticles were synthesized in the existence of montmorillonite in the ratio of dual matrices. They found that the formation of cross-linked carboxymethyl increased the absorption rate.

Srithar et al. (2016) experimentally studied stand-alone triple basin solar still with cover cooling and a concentrator. A concentrator is placed at the bottom surface to reflect the solar radiation to the base of the still. Cover cooling was also done over the top surface, and it was powered by using PV panels. The results showed that the triple basin still has higher efficiency than the CSS, nearly 34.5%. Experimental investigation on v-corrugated absorber CSS using PCM was studied by Shalaby et al. (2016). They used corrugated wick on the basin of the still, and PCM was used as an energy storage material, and it was placed on the basin of the still. The copper tubes were made to flow through to preheat the water between the wick structures. On the other hand, to maintain the heat inside the still, high insulating materials were used on the outer surface of the still instead of polystyrene foam insulation. It also maintained the maximum heat inside the still. Therefore, the productivity of the still was enhanced to around 12% than the CSS. Shyora et al. (2019) made a comparative analysis of stepped still and the CSS. The black absorbing material was placed on the stepped type plates. In addition to this, internal reflectors were placed vertically on the still that improved its evaporation rate. Therefore, stepped still with internal reflectors enhanced the evaporation rate, and the distillate yield was obtained to be 2.770 L/day. The effect of various absorbing materials to improve the output of the still was studied by Abdallah et al. (2009). Materials were used on three different stills and for comparison the fourth still taken is CSS. It has been observed that the wiry sponges have absorbing properties. The results revealed that still with coated metallic

wiry sponges improved the yield to 28%, whereas the uncoated metallic sponges enhanced the yield to 40%, and the volcanic rocks increased the yield to 60%. Therefore, the volcanic rocks are more efficient than the wiry sponges.

Rajaseenivasan and Srithar (2017) experimentally investigated a bubble column humidification and dehumidification module, powered by biomass energy instead of solar energy. The air is flown through a bubble pipe, and it is heated using a preheater, and then flown on the humidifier. The humidifier exchanges the heat to the still, and the exhaust gas is taken out through the dehumidifier pipe. The cold water is pumped through means of a pump, and it is sprayed on the dehumidifier pipe for cooling the system. In this system, the air is heated by recovering the waste heat from biomass stove. Due to this, the distillate was increased to 6.l L/day. Suresh and Shanmugan (2019) studied the effect of water flow in still using novel materials. They used novel materials, e.g., a fin with cotton, fin with jute, and paraffin wax as PCM. The cotton fin and the jute fin were placed on the basin of the still, and it was used as an absorbing material. Therefore, using a fin with cotton wick enhanced the efficiency of around 70.02% than the fin with jute wick materials. The distillate production of the still was 9.429 kg/m^2.

A review of different methods used to augment the output of the stepped solar still has been studied by Kabeel et al. (2015) and found that stepped solar still needs a pump and electrical power for its operation.

In order to eliminate extra power and pump requirements in this study, a novel stepped absorbable plate has been incorporated in the CSS maintaining constant basin water depth. The present study investigates how to improve the distilled water productivity from single slope stepped absorbable plates. The CHEDZ was formed by chitosan, EDTA, and *Chrysopogan zizniodes* and proved to be a super water-retaining material. At the same time, *Chrysopogon* also has some medicinal uses, and it is used in removing the foul smell. The absorbable plate is used to retain water. It has high durability and swelling capacity. Therefore, the performance of PSS using novel absorbing material was studied and comparison of the PSS and CSS is carried out. The paper is structured as follows: the "Experimental setup and methodology" section presents the experimental setup and methodology; the "Durability and cost analysis" section the durability and cost analysis; Methods used for analysis is investigated in the "Methods used for analysis" section; the "Results and discussion" section discusses the formulated results and discussion; the "Comparison of yield of different solar stills" section summarizes the comparative analysis in terms of yield with earlier similar works; finally, the "Conclusions" section highlights the main conclusions of the detailed work.

Experimental setup and methodology

Experimental setup

The schematic and experimental diagrams of the PSS and CSS are shown in Fig. 1 and Fig. 2, respectively. Two single slope stills (one is CSS and other is stepped plates) were taken and correlated for active and passive still for the productivity of freshwater. The dimensions of the PSS and CSS are 0.60 × 0.50 × 0.09 m for both. The experiment was carried out in Kamaraj College of Engineering and Technology, Tamilnadu, India (*9.5° N latitude and 77.96° E longitude*). The side walls of the still are coated with black paint to absorb the heat. Inlet water and freshwater is collected through the inlet and outlet pipes. Distilled water was collected in the 3-mm thickness glass. The polystyrene foam acts as a better insulating material. Therefore, the side walls of the still are covered with polystyrene foam. The PSS is coated with absorbing material, which is formed by the combination of chitosan, EDTA, and *Chrysopogon zizaniodes*. The absorbing material is used to retain the water on the steps. The water on the basin of the PSS is circulated through a DC pump to the saline tank. A low amount of water gets retained on the absorbing material, so evaporation occurs rapidly. The temperatures of basin surface, water, and glass are measured using a digital thermometer with respect to time. The research is carried out from 09:00 am to 17:00 pm, and the readings were noted from December to February 2020. The hourly variations of solar intensity range 700–800 W/m^2, and the daily mean solar intensity of the day taken is 768 W/m^2.

Materials preparation

Preparation of chitosan

The preparation of chitosan is as follows (Boudouaia et al. 2019): During the commencing stage, shrimp fish shells were scrubbed completely with distilled water and then dehydrated to eradicate waste water. The dehydrated fish shells were reduced using 1 normal HCL at a normal temperature of around 30 °C for a period of about 6 h. The reduced slag was cleaned with distilled water until the pH turns around 6–7. The demoralized fish shells were scrutinized in 3.5% NaOH solution at 65°C for 2 h, and discoloration was compassed with NaOCl solution. The obtained samples were washed completely with pure water, and the pH value was calculated, being around 6–7. The resultant chitin was further dehydrated and de-acetylated with 50% NaOH solution 100°C, and treated for 5 h incubation. It is further dissolved in 1% aqueous acetic solution with mechanical stirrer to obtain homogeneous viscous pale yellow solution. Finally, the resultant chitosan was washed completely with freshwater, and the pH value was measured, and the range was around 6.5 and 7.5.

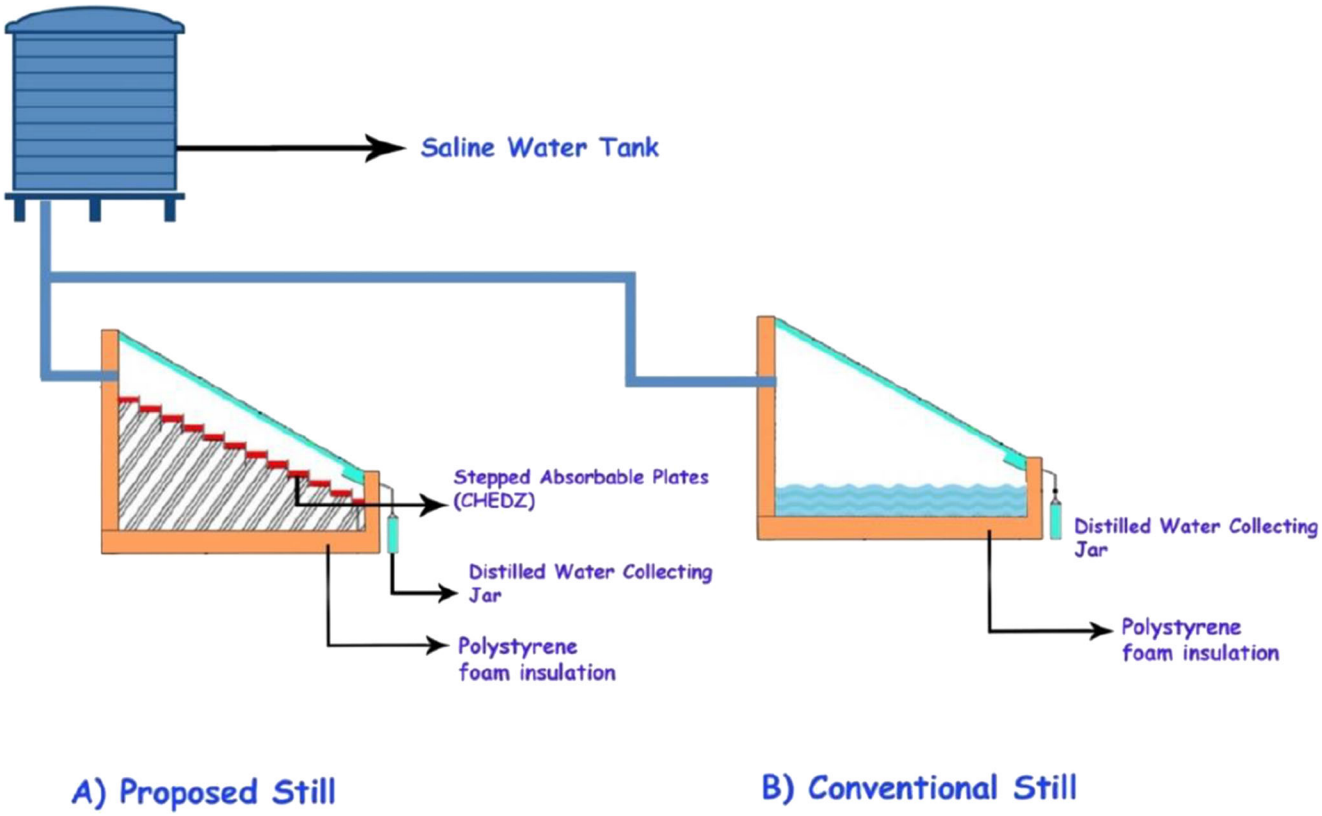

Fig. 1 Schematic drawing of the PSS and CSS. **A** Proposed still. **B** Conventional still

The chemical structure of chitosan is depicted in Fig. 3. The viscosity of the substrate is given as 20–300 cP at 1 wt.% in 1% acetic acid under standard room conditions. The chitosan (molecular weight : 3800–20,000 Da) powder of around 6 g was taken, and it was weighed in a glass beaker and blended with 5 mL of 1% acetic acid solution and stored for about 30 min to get completely dissolved. It was then adulterated with 100 mL distilled water and stirred at 25°C for around 1 h. Various concentrations of chitosan 0 to 1 g at 100 mL of water were added under stirring. Therefore, the chitosan powder was obtained after stirring at a speed of around 100 rpm. The degree of substitution (DS) of the chitosan was premeditated as 0.746, using DD value of chitosan through the following Eq. (1) (Sabaa et al. 2015),

$$DS\% = (7/12 \times (C\%/N\%) + DD{-}4) \times 100 \quad (1)$$

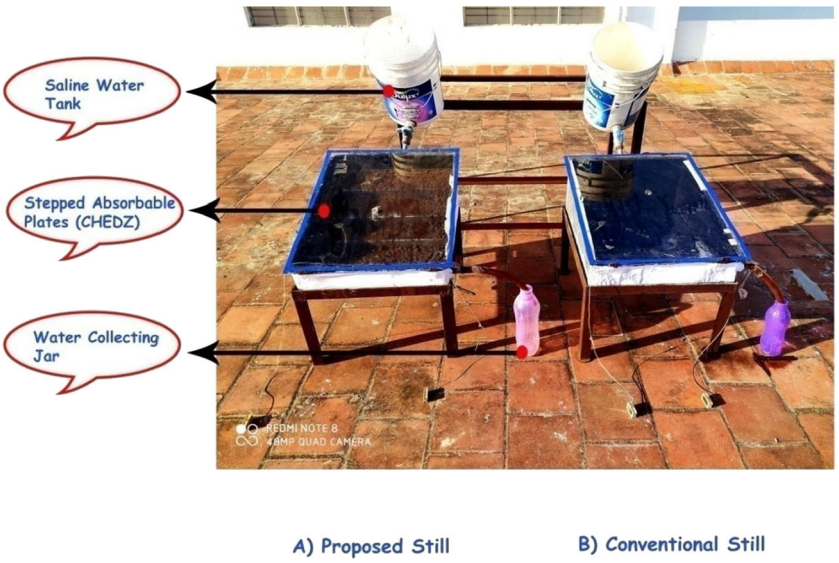

Fig. 2 Photographic view of the PSS and CSS. **A** Proposed still. **B** Conventional still

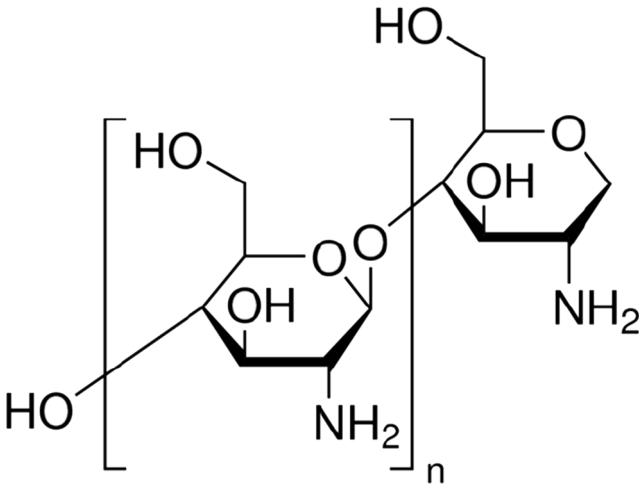

Fig. 3 Structural formula of chitosan

Preparation of CHEDZ

The CHEDZ composite film preparation is as follows (Xu et al. 2005): The obtained chitosan powder of 6 g was taken, and 3 g of *Chrysopogon zizaniodes* (Vetiver) was used. The chitosan powder was immersed in 20 g of HCL solution for 5 h, and the chitosan powder was formed into a gelatine precipitate. Viscous pale yellow solution was obtained. The obtained gelatine was mixed with *Chrysopogon zizaniodes*, and the combination of these two samples EDTA solutions was used to form a cross-linking agent. Therefore, the super absorbent water-retaining material was formed, and it was named CHEDZ. The schematic diagram of CHEDZ preparation is given in Fig. 4.

Super absorbent polymer (chitosan, EDTA, *Chrysopogon zizanioides*)

Super absorbent polymer differs from other types of polymer because the superabsorbent polymer has more water absorbing and retaining capacity; therefore, the superabsorbent polymer is largely used in the production of diapers and napkins. In a recent study, the superabsorbent polymer is used in agricultural lands for retaining water during the rainy season and utilizes the stored water during the time of drought. The water is used for plant growth, giving better plant growth compared to other processes. The super absorbent polymer can be prepared from many materials but, in the present study, the superabsorbent polymer was prepared from waste shrimp shells and natural products: Chitosan, EDTA, and *Chrysopogon zizaniodes*. The obtained super absorbent polymer was coated on steps of the PSS, and it is compared with the CSS.

Solar absorbability The solar absorbability property of chitosan shows a new developed absorption band at 300 nm with alteration in spectrum. Chromophores at 250 nm band of absorption were degraded and new chromophores are generated near 300-nm wavelengths. This increase in absorbance after irradiation is suggested due to the increase in the formation of new carbonyl and amino groups within chitosan (Sionkowska 2006). A new parameter called optical efficiency (Wang and

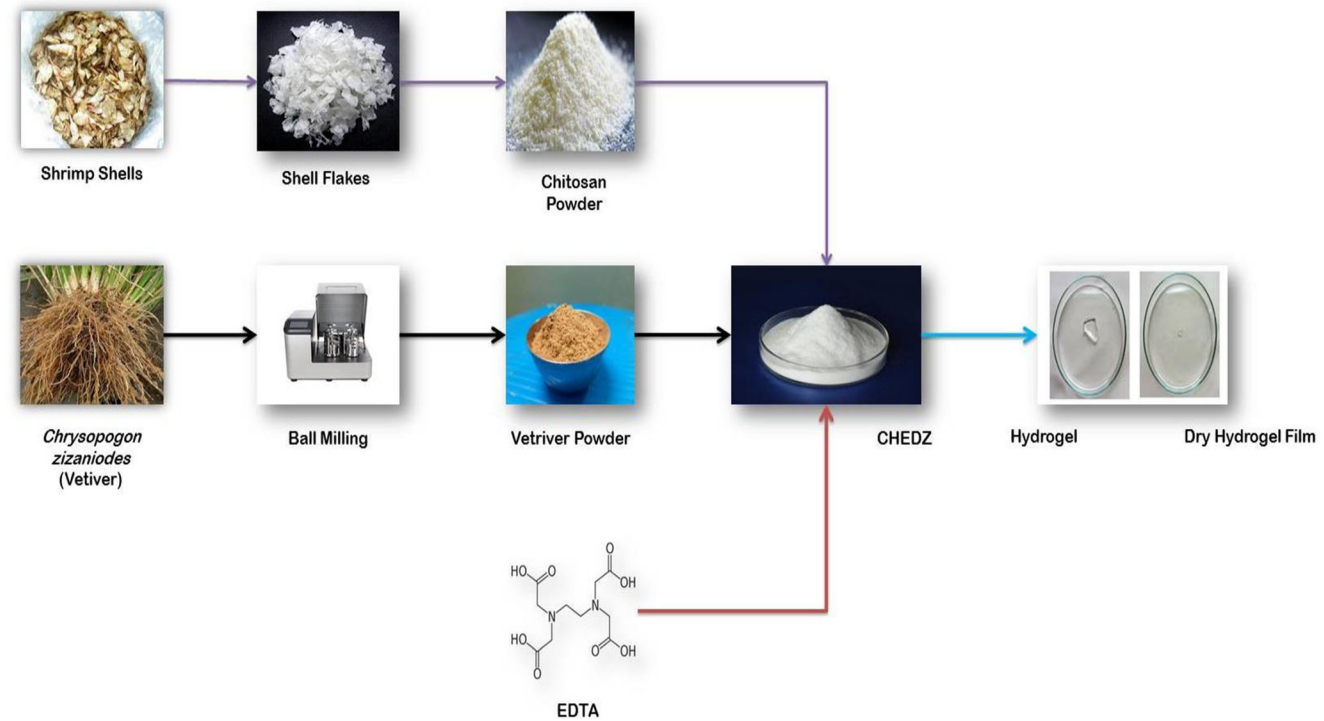

Fig. 4 CHEDZ preparation

Laumert 2017) was analyzed for receiver materials with respect to their designs. This gets influenced with the number of cavity surfaces. The study confirms that surface cavity can increase optical efficiency up to 90%. Chitosan material with cavity surface is capable to increase solar absorbability in terms of optical efficiency.

Swelling capacity The swelling capacity of hydrogel chitosan was earlier discussed in Ritonga et al. (2019). The swelling capacity of the polymer hydrogel is calculated by using known weight of completely dry sample (W1) and 10 mL distilled water (sink sample) (W2) at room temperature for 24 h. Swelling capacity (SC) % is calculated as 110.59%, by using Eq. (2),

$$\mathrm{SC}\% = \frac{W2-W1}{W1} \times 100 \tag{2}$$

where

W1 weight of dry sample
W2 weight of wet sample

The swelling capacity of the material influences the properties of water absorption and condensation in stepped absorber plates. The overall efficiency can increase up to 6% by the implementation of CHEDZ material.

Methodology

The PSS has stepped type arrangement; it is called step type solar still. The construction and dimension of the PSS are similar to the CSS, but in PSS, solar still, internal steps are added. The size of each plate is 0.13 × 0.50 m. The main purpose of the steps in the PSS is to carry and hold the water by using absorbing materials (CH-chitosan, ED-EDTA, Z-*Chrysopogan zizaniodes*). The novel proposed system improves the efficiency of the system (PSS) than compared to the CSS.

Measuring devices

The experiment has suitable instruments to calculate the temperature value of the solar still at different points with respect to time, ambient temperature, wind velocity, solar radiation, and the total amount of yield (output drinking water).

Temperature measuring devices The various temperatures are measured by digital thermometers PM-10 (ranges from −50 to 110°C). The temperature increases during peak time at noon and, thus, the freshwater productivity increases, and the efficiency of solar still also increases. The five digital thermometers were used to measure the basin water temperature, side wall temperature, inner glass temperature, outer glass temperature, and the atmospheric temperature. These temperatures were collected for every hour from 09:00 am to 05:00 pm, and it is used for theoretical calculations.

Wind velocity The wind velocity is measured using an anemometer every hour. In the work area, the velocity of wind ranges between 2 and 7 m/s.

Solar radiation The intensity of solar radiation was measured by using a pyranometer. It measures solar radiation from the sun in W/m^2. In this study, the intensity of solar radiation ranges between 0 and 1.1 kW/m^2.

Assumptions:
- The brackish water is fed to the still continually.
- The level of the water was maintained constant in both stills.
- The evaporative losses are reduced because the stills are covered by the insulating materials.
- The direct and scatter radiation received from the sun is absorbed by the glass cover.

Uncertainty analysis

Several parameters need to be measured during the experiment. These parameters are inside and outside still glass temperature, basin sidewall temperature, basin water temperature, environmental temperature, wind speed, solar intensity, and quantity of output distilled water. Table 1 gives the tabulated correctness of uncertainty for measuring instruments used. In general, for any parameter h, calculated or measured directly from the experiment, the uncertainty h given as σ_h could be obtained by Eq. (3) as given below (Sohani et al. 2021),

$$\sigma_h = \sqrt{\left(\frac{\partial h}{\partial x}\right)^2 \sigma_x{}^2 + \left(\frac{\partial h}{\partial y}\right)^2 \sigma_y{}^2} \tag{3}$$

where

σ_x and σ_y are the known uncertainty values of x and y parameters either measured directly or calculated.
$\frac{\partial h}{\partial x}$ *and* $\frac{\partial h}{\partial y}$ are their corresponding partial derivatives.

The dimensions of the solar still are measured directly using measuring tape and steel scale with a correctness of ± 0.1 cm and ± 1 mm respectively.

Thermocouple temperature sensor The temperature measurement is carried out by using a Digital Thermometer PM-10. The thermocouple temperature sensor was used to measure

Table 1 Correctness of discrete measuring instruments

S. No.	Instrument	Accuracy	Range	Standard uncertainty
1	Anemometer	± 0.1 m/s	0–15 m/s	0.05 m/s
2	Thermocouple	± 0.1 °C	0–100 °C	0.05 °C
3	pH meter	± 0.01	0–14	0.005
4	Pyranometer	± 1 W/m^2	0–5000 W/m^2	0.57 W/m^2
5	Distilled water flask	± 0.5 mL	0–2 L	0.28 mL

still temperature; ranged −50 to 110 °C with an accuracy of ± 1 °C. It is also observed that the temperature increases until noon with increase in still performance. The thermocouple is used to measure various parameters like

- Outer glass temperature
- Inner glass temperature
- Atmospheric temperature
- Side wall and CHEDZ temperature
- Basin water temperature

Anemometer The wind speed was measured by an anemometer, ranged from 0 to 15 m/s by the correctness of ± 0.1 m/s.

Pyranometer The solar ray intensities of radiation are calculated by using a pyranometer, ranged 0–1.2 kW/m^2 with a correctness of 1 W/m^2.

Water quality The distillate yield was calculated by a storage tank, which has various levels for measuring the level of the water and the capacity of the tank ranges between 3 and 4 L. Water quality was analyzed and tested in the water testing chemical laboratory. The different compound variables of the water sample are experienced and analyzed. pH value was determined by the pH meter, which is ranged from 0 to 14.

Uncertainty calculation of measured parameters

Solar still area (A) Area of still (A) is given by,

$$A = l \times w$$

$\frac{\partial A}{\partial l} = w$ and $\frac{\partial A}{\partial w} = 1$

By using the proposed uncertainty equation from Panchal and Sathyamurthy (2020),

$$\frac{\omega_A}{A} = \sqrt{\left(\frac{1}{A}\frac{\partial A}{\partial l}\omega_l\right)^2 + \left(\frac{1}{A}\frac{\partial A}{\partial w}\omega_w\right)^2}$$

$$\frac{\omega_A}{A} = \sqrt{\left(\frac{\omega_l}{l}\right)^2 + \left(\frac{\omega_w}{w}\right)^2}$$

$$\frac{\omega_A}{A} = \sqrt{\left(\frac{0.001}{1}\right)^2 + \left(\frac{0.001}{1}\right)^2}$$

$$\therefore \frac{\omega_A}{A} = 0.0014 \text{ (or) } 0.14\%$$

Durability and cost analysis

The durability of material used can be affected by wetness of the isolated environment (basin) (Prakash and Velmurugan 2015). Table 2 depicts the durability comparison in years. The comparison between CSS and PSS is depicted in Fig. 5.

The overall cost of the PSS and CSS includes the cost of manufacturing, cost of insulating material, cost of measuring equipment, cost of absorbing materials, and other contingencies (Balachandran et al. 2021a). The labor cost and other cost depend on the size of the desalination unit. The construction of the system is simple; therefore, it requires less maintenance cost (Balachandran et al. 2020b). It is also inferred that PSS has faster payback period in comparison to CSS. The fabrication cost of stepped absorbable plate using aluminum including the preparation of CHEDZ is calculated nearer to 1000 (in INR). Table 3 lists the cost analysis for the experimental study. Table 4 shows the cost analysis of different types of stills. From Table 4, it is clear that the work produces freshwater at a rate of 0.032 $, which is lower than other types of stills.

$$CRF = \frac{i(1+i)^n}{(1+i)^n - 1} \quad (4)$$

$$FAC = P(CRF) \quad (5)$$

$$SFF = \frac{i}{(1+i)^n - 1} \quad (6)$$

Table 2 Durability comparison (in years)

Items	CSS	PSS
Glass cover	5	6
CHEDZ stepped absorber plate	-	2

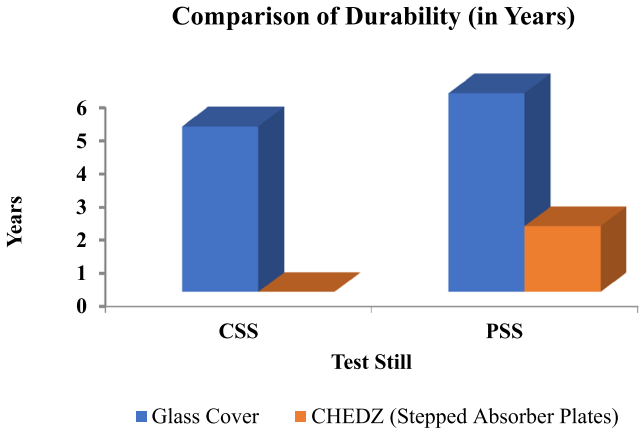

Fig. 5 Comparison of durability (in years)

$$ASV = S(SFF) \tag{7}$$

$$AC = FAC + AMC - ASV \tag{8}$$

$$CPL = \frac{AC}{M} \tag{9}$$

$$S = 0.2P \tag{10}$$

$$AMC = 0.15\ FAC \tag{11}$$

$$\text{Net Profit} = \text{Water Production cost} - \text{Maintenance cost} - \text{Feed Water cost} - \text{Operational cost.} \tag{12}$$

where

CRF	Capital Recovery factor
P	Present capital cost
FAC	Fixed annual cost
S	Salvage value
SFF	Sinking fund factor
ASV	Annual salvage value
AMC	Annual maintenance operation cost
AC	Annual cost
M	Average annual capacity
CPL	Cost per liter (Shalaby et al. 2016; Balachandran et al. 2020a)..

Table 3 Cost analysis

Particulars	CSS	PSS
Investment on still design and maintenance (cost in)	6500	7500
Feed water (cost in)	15	15
Yield (L/m^2/day)	2.47	3.05
Revenue/day	37.05	45.75
Payback period (in days)	175	164

Methods used for analysis

Table 5 shows the main parameters employed on the PSS design.

Analysis of energy

The thermodynamics laws are used to analyze the energy rate at the fundamental step. The energy balance equation for the stable flow operation of an open system is explained below. The energy and exergy efficiency of the PSS and CSS has diverse actions depending on climatic and operating environment. The energy efficiency of the PSS and CSS is defined by heat losses from water to the overall net energy received from collector surface of the PSS and CSS (Caliskan 2017; Manokar et al. 2018; Balachandran et al. 2020a).

$$En_{w,in} + En_{solar,in} = En_{w,out} + En_{loss} \tag{13}$$

$$\Delta En_w = En_{w,out} - En_{w,in} = m_w c_p \left(T_{w,out} - T_{w,in}\right) \tag{14}$$

$$En_{solar,in} = \alpha q A \tag{15}$$

$$En_{loss} = Q_{loss,conv} + Q_{loss,rad} \tag{16}$$

$$Q_{loss,rad} = \epsilon \sigma A \left(T_{sur}{}^4 - T_{air}{}^4\right) \tag{17}$$

$$Q_{loss,conv} = hA\left(T_{surf} - T_{air}\right) \tag{18}$$

$$h = \frac{kNu}{L} \tag{19}$$

$$L = \frac{A}{P} \tag{20}$$

$$Nu = (0.15)Ra^{1/3} \tag{21}$$

$$Ra = \frac{gcoscos\ \left(T_{surf} - T_{air}\right)L^3 Pr}{v^2} \tag{22}$$

$$n = \frac{\Delta En_w}{En_{solar,in}} \times 100 \tag{23}$$

Exergy analysis

The exergy equilibrium for any process can be derived from law of conservation of energy and second law of thermodynamic. Energy analysis provides a perceptible view of energy successfully applied to the system. On the other hand, exergy efficiency offers a higher potential useful energy that can be obtained from the solar still. The exergy efficiency of the CSS and PSS is given by exergy output of desertion to the exergy input to the CSS and PSS (Ranjan and Kaushik 2013; Balachandran et al. 2021b).

$$Ex_{w,in} + Ex_{solar,in} = Ex_{w,out} + Ex_{loss} + Ex_{dest} \tag{24}$$

Table 4 Relative expenditure breakdown for different stills

Solar still	P	CRF	FAC	S	SFF	ASV	AMC	AC	M	CPL	Reference
Transportable hemispherical wick	190	0.177	34	38	0.057	2	5	37	585	0.063	(Kabeel et al. 2010)
With pin finned wick	280	0.177	50	56	0.057	3.2	7.5	54.3	1001	0.054	(Kabeel et al. 2010)
With sponge and pond	250	0.177	44.3	50	0.057	3	6.6	47.9	731	0.065	(Kabeel et al. 2010)
With a shallow solar pond	122.5	0.177	21.68	24	0.057	1.4	3.25	23.54	910	0.025	(El-Bialy et al. 2016)
Single slope	94	0.177	16.64	18.8	0.057	1.07	2.5	18.06	681	0.026	(El-Bialy et al. 2016)
With separate condenser	120	0.177	21.24	24	0.057	1.37	3.19	23.06	780	0.029	(El-Bialy et al. 2016)
With fin type	160	0.177	28.32	32	0.057	1.82	4.25	30.74	429	0.071	(El-Bialy et al. 2016)
Proposed Still	116.5	0.177	20.62	23.3	0.057	1.32	3.09	22.39	684	0.032	(Present work)

$$\Delta Ex_w = Ex_{w,out} - Ex_{w,in} \tag{25}$$

$$Ex_{w,out} = m_w c_p \left[(T_{w,out} - T_0) - T_0 ln\left(\frac{T_{w,out}}{T_0}\right)\right] \tag{26}$$

$$Ex_{w,in} = m_w c_p \left[(T_{w,in} - T_0) - T_0 ln\left(\frac{T_{w,in}}{T_0}\right)\right] \tag{27}$$

$$Ex_{solar,in} = En_{solar,in}\left[1 + \frac{1}{3}\left(\frac{T_0 + 273}{T_{sun} + 273}\right)^4 - \frac{4}{3}\left(\frac{T_0 + 273}{T_{sun} + 273}\right)\right] \tag{28}$$

$$Ex_{loss,rad} = Q_{loss,conv}\left(1 - \frac{T_0}{T_{surf}}\right) \tag{29}$$

$$Ex_{loss,rad} = Q_{loss,rad}\left(1 - \frac{T_0}{T_{surf}}\right) \tag{30}$$

$$Ex_{dest} = Ex_{w,in} + Ex_{solar,in} - Ex_{w,out} - Ex_{loss} \tag{31}$$

$$S_{gen} = \frac{Ex_{dest}}{T_0} \tag{32}$$

$$\varphi = \frac{\Delta Ex_w}{Ex_{solar,in}}\ x\ 100 \tag{33}$$

$$SI = \frac{1}{1 - \varphi} \tag{34}$$

Table 5 Various parameters used on the design of PSS

Constraint	Representation	Rate
Glass temperature	T_{surf}	46 °C
Air temperature	T_{air}=T_0	38 °C
Average temperature	T_{avg}	35 °C
Sun temperature	T_{sun}	6000 K
Thermal conductivity	K	0.03588 W/m °C
Kinematic viscosity	V	0.00001608 m^2/s
Prandtl number	Pr	0.7282
$\beta = \frac{1}{T_{avg}}$	β	0.00339867 K
Area	A	3 m^2
Perimeter	P	7 m
Characteristic length	$L = \frac{A}{P}$	0.4285714286 m
Collector angle	θ	30
cosθ	cos (30)	0.866025403
Acceleration of gravity	G	9.81 m/s^2
Emissivity	E	0.9
Stefan Boltzmann constant		(5.67) x 10^{-8} W/m^2K^4
Permeability	A	0.88
Solar intensity	Q	660 W/m^2
Mass flow rate of water	m_w	0.0155556 kg/s
Specific heat	c_p	4180 J/kg °C
Water inlet temperature	T_{in}	25 °C
Water output temperature	T_{out}	31 °C

Results and discussion

Performance of the PSS and CSS due to basin water and collector cover temperature

The collector cover temperature shows a crucial aspect of the output of the PSS and CSS as shown in Fig. 6. The different factors such as collector cover, basin, wall, and saltwater temperatures constantly increase and reached their highest value in midday and decrease slowly and reach lowest value in sunset hours. The increases in solar intensity are directly proportional to the rate of increase in collector cover temperature. From 9 am to 12 pm, temperatures increase gradually, and at noon the temperature rises suddenly and attains its peak value at 1 pm. During peak time, the temperature of the glass is 54 °C. After 1 pm, the glass temperature slowly falls down, and during the time of 5 pm the temperature decreases.

The keen observation from Fig. 7 result fair reading of basin temperature taken per hour reaches its peak values at noon. During the time of 9 am, the basin temperature starts increasing gradually. During 12 pm, there is a sudden rise, and the temperature value increases linearly due to the presence of absorbable stepped plates which retain the water on its basin surface. Due to water retention on the PSS, the heat transfer rate increases from the glass surface to the stepped plates of the still. Therefore, the water surface is heated, and the basin gets heated rapidly. At 1 pm, the temperature of the basin of the PSS is around 64 °C, and it is maintained for a short time. Then, the solar radiation starts to decrease, so the temperature of basin water decreases slowly during the evening. During the time of 5 pm, the basin temperature falls down to 45 °C. The hourly variations of CHEDZ coated still temperature is plotted in Fig. 8. From the graph, it is inferred that the CHEDZ retains heat until evening with respect to ambient temperature and still temperature.

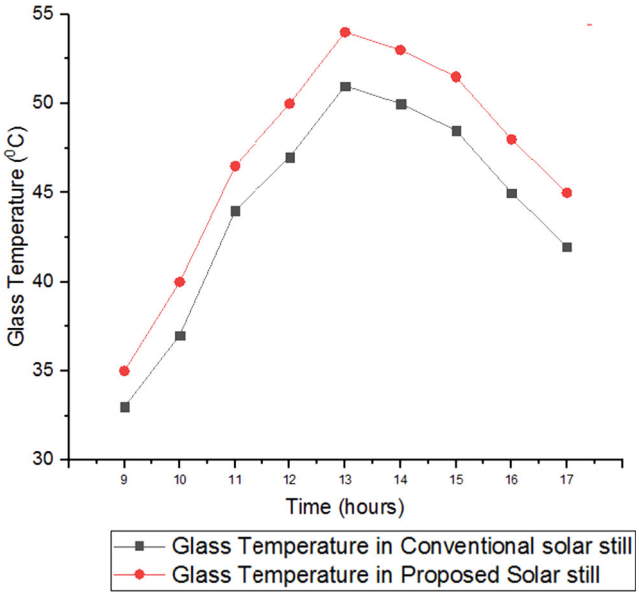

Fig. 6 Hourly variation of glass temperature for the CSS and PSS

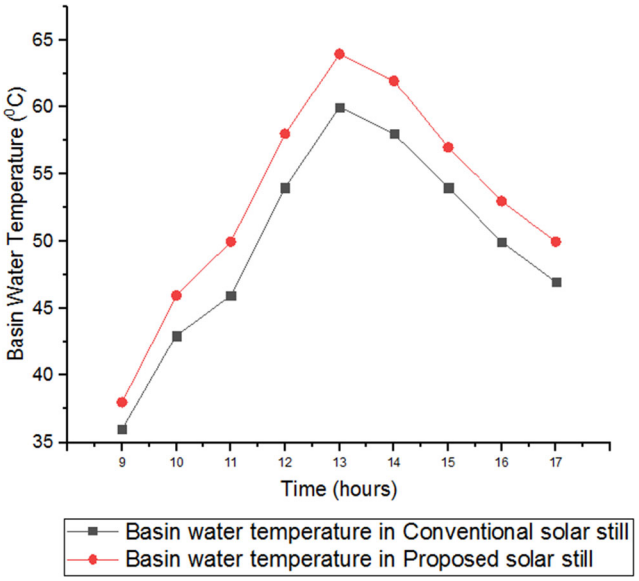

Fig. 7 Hourly variation of basin water temperature for the CSS and PSS

Performance of PSS and CSS due to the effect of solar intensity, wind velocity, and ambient temperature

The keen observation from the result shows that the reading of hourly solar intensity reaches its peak values at midday. The graph also shows that temperatures were maintained maximum from 12:00 pm to 02:00 pm. The linear change in the temperature denotes that the temperature decreases gradually in a few hours between 02:00 pm and 05:00 pm. From morning 09:00 am to 02:00 pm, all the temperatures were rising constantly due to solar intensity input to the PSS and CSS. Figure 9 shows the graph of hourly variations of ambient temperature. The atmospheric temperature reaches its

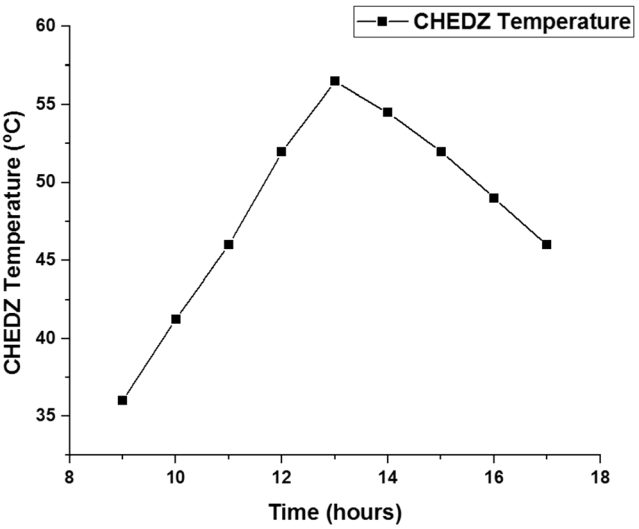

Fig. 8 Hourly variation of CHEDZ temperature

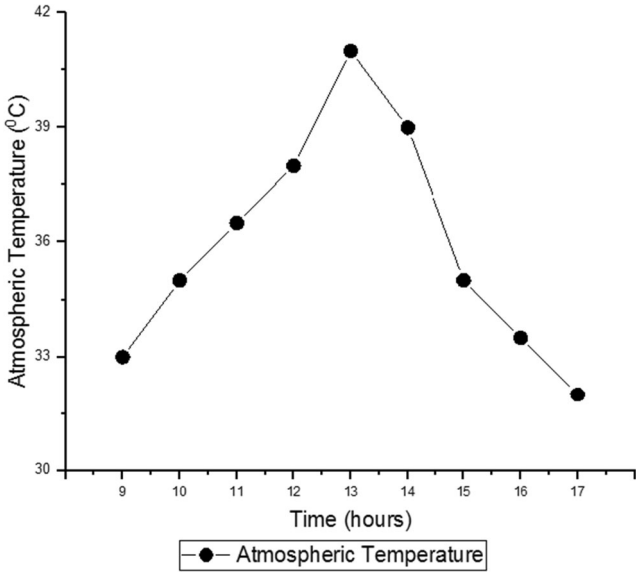

Fig. 9 Hourly variation of atmospheric temperature

maximum value during the noon hour, and the peak value is around 41°C during afternoon. The average value of atmospheric temperature is around 35–38°C. Figure 10 explains the disparity of solar intensity and wind velocity every hour. It is noticed that from the figure, both solar intensities (1100 W/m^2) reach a peak on 01:00 pm. After 1:00 pm, solar intensity starts to decrease gradually due to the receiving of IR radiation.

The productivity of solar still depends on wind velocity to a certain extent. Beyond which wind velocity remains insignificant towards yield. It is also noted that yield of the still increases by 35% when wind velocity changes from 2.7 to 5 m/s (Badran 2007). Yield starts to decrease by 13% between the range of 9 m/s (Nafey et al. 2000; Kabeel et al. 2015). Wind velocity at higher range may also affect evaporative and convective heat transfer coefficients (Nafey et al. 2000). Figure 7 shows the hourly variation of wind velocity with respect to time. For the particular test day, the wind velocity is maximum with 6.5 m/s at around 5 PM. By 1 PM, the yield increases to its peak with ambient wind conditions. Figure 10 depicts the experimental variation that is studied in comparison between CSS and PSS with respect to wind velocity (Fig. 11).

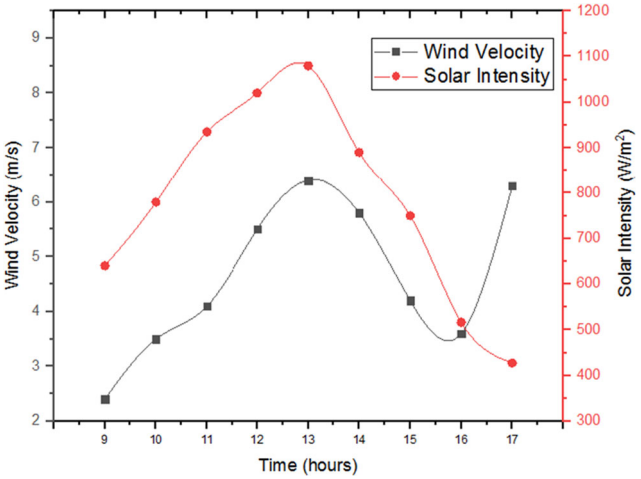

Fig. 10 Hourly variation of wind velocity and solar intensity

Effect of water depth

The yield productivity strongly depends on parameters like intensity, constant depth, and geometry of the basin. Various literature studies have investigated the effect and impact of water depth in the still and reported that maintaining constant depth throughout the experiment gives high efficiency. It is evident that yield increases with minimum water depths. The determination of optimal water depth may increase reasonable still performance. Furthermore, increase in basin water decreases output yield (Jamil and Akhtar 2017).

However, maintaining a water depth constantly for every hour is assumed for enhancing the yield. During maximum intensity with constant depth, the temperature of water inside the basin may increase up to 20%. This happens with respect to increased basin temperature (Kumar et al. 2017). Earlier investigation on stepped solar still has brought a greater productivity yield of 6.7 L/day considering lower depth. The variation in evaporation rate was observed mildly in conventional stills and high for stepped stills. Hence forth, it is suggested to ensure minimum constant depth has low volumetric heat capacity so as to increase heat transfer capabilities (Alaudeen et al. 2014). This infers that yield productivity directly relies on solar irradiation and inversely proportional to the depth of water (Sathyamurthy et al. 2014). Thus, yield can be increased up to 57.8% in response to constant depth (Kabeel et al. 2012).

Effect of absorbing material on yield

Figure 12 gives hourly variation of yield from the CSS and PSS. As solar intensity increases from sunrise hours to midday, yield increases during these hours and reaches a

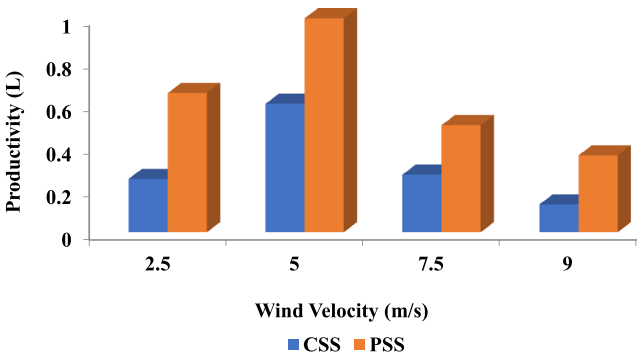

Fig. 11 Variation of productivity with respect to wind velocity

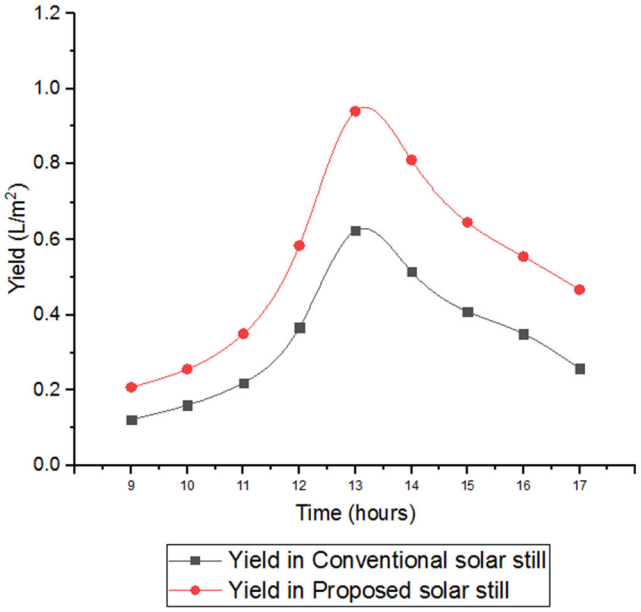

Fig. 12 Hourly variation of the yield from the CSS and PSS

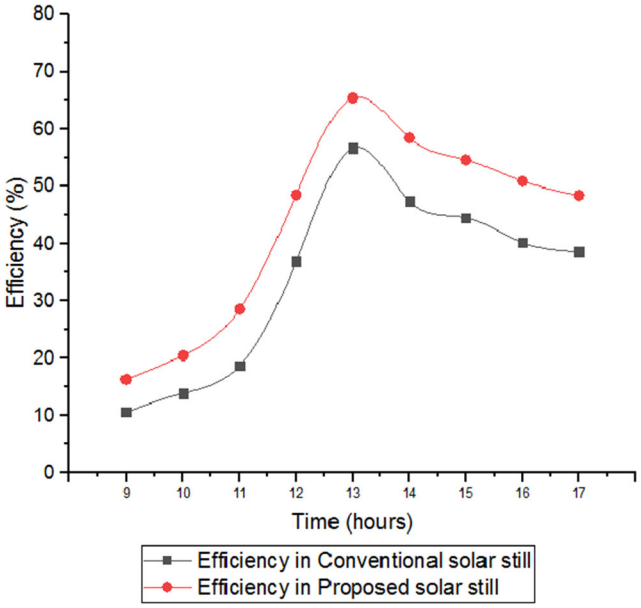

Fig. 13 Hourly variations of thermal efficiency for the CSS and PSS

maximum around noon hours and starts decreasing because the solar intensity also decreases and reached minimum value during the sunset hours. Furthermore, it is noted that both freshwater production and water temperature reach their maximum during the same time. The freshwater obtained during the initial stage was minimum. The highest amount of freshwater was obtained from 11:00 am to 15:00 pm. The maximum output of 1 L/m^2 was obtained during the peak hours from the PSS. The yield from the CSS was 0.6 L/m^2, obtained during peak hours. Due to water-retaining material coated on the stepped plates, the productivity of water was increased during peak hours at 01:00 pm, which is much more than the CSS. The higher output was produced from the PSS than the CSS as the evaporation rate on PSS is increased due to higher basin water temperature on the PSS. The cause for the consistent augment in water temperature is due to that a very few amounts of water present on the steps which get evaporated quickly. Maximum difference was 0.4 L/m^2 between two stills in the peak hours, and distillate yield was more in the PSS than the CSS. The aluminum steps are used to transfer the heat to water retaining on the steps of the PSS. By using a super water-retaining material, the evaporation rate would increase and, thereby, the distillate output would be more.

Thermal efficiency analysis of PSS and CSS

Figure 13 represents the hourly thermal efficiency variations of the PSS and the CSS. For CSS, the value of thermal efficiency at 09:00 am was 10.67%, which is minimum due to the low amount of solar intensity, and during the evening at 17:00 pm the thermal efficiency was 38.66%. For the proposed, the value of thermal efficiency at 09:00 am was 16.37%, which is minimum due to the low amount of solar intensity, and during the evening at 17:00 pm thermal efficiency was 47.5%. At 17:00 pm, efficiency is higher than morning hours because the output constantly takes place even later than the sunset hours.

Rate of energy, rate of exergy, and efficiency of energy rate and exergy rate

Net energy rate is the amount of energy input rate of water with losses. The incoming energy rate, loss rate, and energy in the nature of heat are 1728, 735, and 358 W, respectively. The

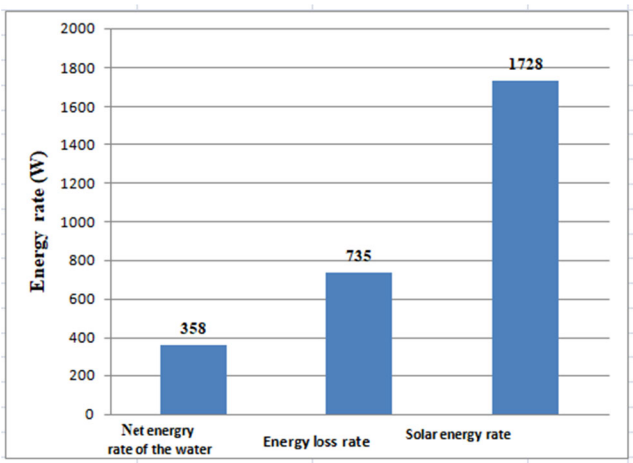

Fig. 14 Analysis of various energies of solar still

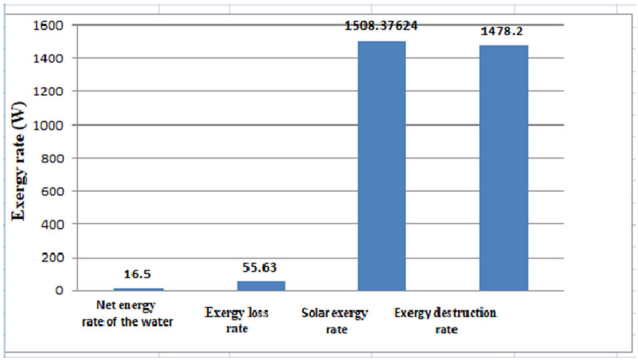

Fig. 15 Exergy analysis results

input energy lost is because of convection and radiation. Radiation heat losses are the major loss compared with convection losses because the entire system is operated by solar energy, which mainly depends on the heat transfer mechanism (Caliskan 2017). The rate of augment in energy efficiency is based on heat transfer rate from the stepped plates to basin water surface, which enhance distilled water output. The energy efficiency of the PSS is 18.34% higher than the CSS as listed in Fig. 14.

The exergy rate analysis is a comparison between net energy rate of water, energy loss rate, solar exergy rate, and exergy destruction rate. From this, the incoming rate is calculated as 16.5, 55.63, 1508.37, and 1478.2 W, respectively. From the experimental setup, the energy efficiency is found to be 18.34%, and the exergy efficiency is found to be 0.45%. Therefore, from the results as listed in Fig. 15, it was observed that the efficiency of the energy rate is higher than the efficiency of the exergy rate.

The efficiency of the system is shown in Fig. 16. The energy efficiency rate of the system is estimated to be 18.34%, whereas the exergy efficiency is determined by 0.45%. This shows that exergy is the available energy, and it is associated with the environmental conditions of the system. It reports that exergy is a useful part, and a maximum of it is destructed due to irreversibility.

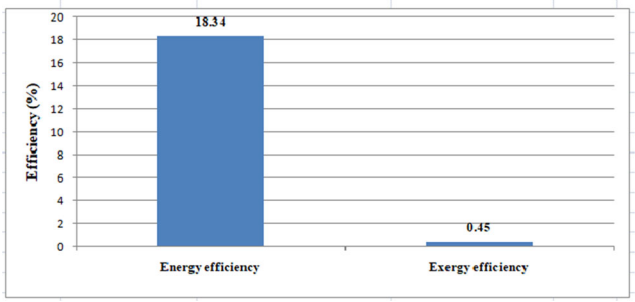

Fig. 16 Efficiency results of energy and exergy rates

Table 6 Comparison of different methods

S. No.	Experimental work done	Yield	Reference
1.	CSS with pin finned wick materials	3.15 L	(Alaian et al. 2016)
2.	Enhancing the performance of the CSS using film cooling and hybrid composite insulation	1.42 L	(Balachandran et al. 2020)
3.	CSS with various wick elements	3.03 L	(Bhargva and Yadav 2019)
4.	CSS with various basin materials	1.880 L	(Gnanaraj and Velmurugan 2019)
5.	Enhancing the output of double slope still using phase changing materials	4.34 L	(Khandagre et al. 2019)
6.	Performance enrichment of the still using efficient heat exchange mechanism	4.53 L	(Kabeel et al. 2017)
7.	Performance of the still by salt rejecting floating solar still	2.5 L	(Ni et al. 2018)
8.	Performance analysis of dual slope wick still	4.50 L	(Pal et al. 2017)
9.	Enhancement of the still by integrating evacuated tubes	8.1 L	(Patel et al. 2019)
10.	Performance enhancement of the still by triple basin still with cover cooling and parabolic dish concentrator	2.75 L	(Srithar et al. 2016)
11.	CSS with stepped absorbable plates	3.05 L	Present study

Comparison of yield of different solar stills

The comparison of yield of CSS using novel materials is summarized in Table 6. The output is higher in the case of integrating evacuated tubes in the solar still. The comparison of yield mainly depends on the type of material used in the solar still, and it is used to augment the output. In the present study, a solar still desalination by using a novel super absorbing material which consists of chitosan, EDTA, and *Chrysopogon zizaniodes* has produced the maximum yield of 3.05 L/day.

Conclusions

In the present study, water desalination is done on absorbable stepped plates using novel absorbing materials, and it is tested under Indian climatic conditions. Mohammed (2013) mentioned a 75% rise in productivity with stepped plates and using reflectors. Alaudeen et al. (2014) also concluded that PSS with stepped plates increased the productivity to 16% with respect to CSS. Therefore, two stills have been designed, one with stepped absorbable plates and the other with conventional CSS. The absorbing material has a high tendency to retain more amount of water. In addition to this, the water on the basin surface of the still is circulated using a DC motor.

- The distillate water is taken, and it is measured by the pH meter, and it is compared with the standard water quality. The results revealed that the water is toxic-free, and it is safe for drinking purposes.
- The distillate yield of the PSS was obtained to be 3.05 L/day, whereas the yield of the CSS is 2.47 L/day.
- The proposed still produces a maximum yield of 0.98 L during 01:00 pm, while the CSS produce a maximum yield of 0.57 L.
- The thermal efficiency of still reaches its maximum in the noon time between 12:00 pm and 13:00 pm, and the peak value attained is 65.46%.
- Both stills are covered using polystyrene foam insulation and, therefore, act as a perfect insulating medium.
- The waste shrimp fish shells were taken, and it is used for the preparation of chitosan, and it acts as a better absorbing material.
- The *Chrysopogon zizaniodes* is used along with the absorbing material. It helps in removing bacterial accumulation, and it is used to remove bad odor.
- In comparison with the CSS, the PSS are close to the top surface, and the losses are less from reaching the glass surface to the basin surface, and it is used for improving the efficiency of the PSS.

Abbreviations EDTA, ethylene diamine tetraacetic acid; CHEDZ, composed of chitosan (obtained from waste shrimp shells), ethylene diamine tetraacetic acid (EDTA), and *Chrysopogon zizaniodes*; PSS, proposed solar still; CSS, conventional solar still**Nomenclature** $En_{w,in}$, energy input rate of the water; $En_{solar,\ in}$, solar energy input rate; $En_{w,\ out}$, energy output rate of the water; En_{loss}, energy rate of the system; α, permeability of the system; q, solar radiation rate and collector area; A, area; En_{loss}, energy loss rate of the system; $Q_{loss,\ conv}$, convection heat loss rate; $Q_{loss,\ rad}$, radiation heat loss rate; ϵ, emissivity of the system; σ, Stefan Boltzmann constant; h, convection heat transfer coefficient; T_{surf}, slass surface temperature; T_{air}, air temperature; k, thermal conductivity; Nu, Nusselt number; L, characteristics length of the system; Ra, Rayleigh number; G, perimeter; Pr, Prandtl number; v, kinetic viscosity; θ, angle of the solar collector; T_0, dead state temperature; T_{sun}, sun temperature; $T_{w,\ in}$, collector input temperature; $T_{w,\ out}$, collector output temperature; m_w, mass flow rate; c_p, specific heat; $\propto$, permeability of the system; $Q_{loss,\ rad}$, convection heat loss rate; $Q_{loss,\ conv}$, radiation heat loss rate; T_{surf}, glass surface temperatures; $Ex_{w,\ in}$, exergy input rater of the water; $Ex_{w,\ out}$, exergy output rate of the water; ΔEx_W, net exergy rate of the water; $En_{solar,\ in}$, solar energy input rate; $Ex_{solar,\ in}$, solar exergy input rate; φ SI, sustainability index; $Ex_{loss,\ rad}$, radiation exergy loss rate; $Ex_{loss,\ conv}$, convection exergy loss rate; Ex_{loss}, exergy loss rate of the system; Ex_{dest}, exergy destruction rate of the system; S_{gen}, entropy generation rate

Acknowledgements The authors would like to thank Alfredo Peinado (Birmingham University, UK) for his detailed revision of the context.

Availability of data and materials Not applicable.

Author contribution Gurukarthik Babu Balachandran: Conceptualization, methodology, software.

Prince Winston David: Data curation, writing — original draft preparation.

Anandha Balaji Alexander: Software, investigation, validation.

Muthu Manokar Athikesavan: Writing — reviewing; formal analysis.

Padmanaban Velayudha perumal Chellam: Editing, project administration.

Krishna Kumar Sasi Kumar: Visualization.

Vinothkumar Palanichamy: Supervision, investigation.

Abd Elnaby Kabeel: Conceptualization, methodology.

Ravishankar Sathyamurthy: Formal analysis.

Fausto Pedro Garcia Marquez: Editing, methodology.

Declarations

Ethical approval Not applicable.

Consent to participate Not applicable.

Consent to publish Not applicable.

Competing interests The authors declare no competing interests.

References

Abdallah S, Abu-Khader MM, Badran O (2009) Effect of various absorbing materials on the thermal performance of solar stills. Desalination 242:128–137. https://doi.org/10.1016/j.desal.2008.03.036

Alaian WM, Elnegiry EA, Hamed AM (2016) Experimental investigation on the performance of solar still augmented with pin-finned wick. Desalination 379:10–15. https://doi.org/10.1016/j.desal.2015.10.010

Alaudeen A, Johnson K, Ganasundar P, Syed Abuthahir A, Srithar K (2014) Study on stepped type basin in a solar still. J King Saud Univ - Eng Sci 26:176–183. https://doi.org/10.1016/j.jksues.2013.05.002

Arunkumar T, Kabeel AE, Raj K, Denkenberger D, Sathyamurthy R, Ragupathy P, Velraj R (2018) Productivity enhancement of solar still by using porous absorber with bubble-wrap insulation. J Clean Prod 195:1149–1161. https://doi.org/10.1016/j.jclepro.2018.05.199

Badran OO (2007) Experimental study of the enhancement parameters on a single slope solar still productivity. Desalination 209:136–143. https://doi.org/10.1016/j.desal.2007.04.022

Balachandran GB, David PW, Chellam PV, Ali MNA, Radhakrishnan V, Balamurugan R, Manokar AM (2020a) Rehash of cooked oil for the palatable water production using single slope solar still. Environ Sci Pollut Res 27:117613. https://doi.org/10.1016/j.fuel.2020.117613

Balachandran GB, David PW, Mariappan RK, Kabeel AE, Athikesavan MM, Sathyamurthy R (2020b) Improvising the efficiency of single-sloped solar still using thermally conductive nano-ferric oxide. Environ Sci Pollut Res 27:32191–32204. https://doi.org/10.1007/s11356-019-06661-2

Balachandran GB, David PW, Vijayakumar ABP, Kabeel AE, Athikesavan MM, Sathyamurthy R (2020c) Enhancement of PV/T-integrated single slope solar desalination still productivity using water film cooling and hybrid composite insulation. Environ Sci Pollut Res 27:32179–32190. https://doi.org/10.1007/s11356-019-06131-9

Balachandran GB, David PW, Radhakrishnan V, Ali MNA, Baskaran VK, Virumandi D, Athikesavan MM, Sathyamurthy R (2021a) Investigation on the performance enhancement of single-slope solar still using green fibre insulation derived from Artocarpus heterophyllus rags reinforced with Azadirachta indica gum. Environ Sci Pollut Res. https://doi.org/10.1007/s11356-021-13062-x

Balachandran GB, David PW, Rajendran G, Ali MNA, Radhakrishnan V, Balamurugan R, Athikesavan MM, Sathyamurthy R (2021b) Investigation of performance enhancement of solar still incorporated with Gallus gallus domesticus cascara as sensible heat storage material. Environ Sci Pollut Res 28:611–624. https://doi.org/10.1007/s11356-020-10470-3

Bhargva M, Yadav A (2019) Experimental investigation of single slope solar still using different wick materials: a comparative study. J Phys Conf Ser 1276:012042. https://doi.org/10.1088/1742-6596/1276/1/012042

Boudouaia N, Bengharez Z, Jellali S (2019) Preparation and characterization of chitosan extracted from shrimp shells waste and chitosan film: application for Eriochrome black T removal from aqueous solutions. Appl Water Sci 9:1–12. https://doi.org/10.1007/s13201-019-0967-z

Caliskan H (2017) Energy, exergy, environmental, enviroeconomic, exergoenvironmental (EXEN) and exergoenviroeconomic (EXENEC) analyses of solar collectors. Renew Sust Energ Rev 69:488–492. https://doi.org/10.1016/j.rser.2016.11.203

Chen H, Lin J, Zhang N, Chen L, Zhong S, Wang Y, Zhang W, Ling Q (2018) Preparation of MgAl-EDTA-LDH based electrospun nanofiber membrane and its adsorption properties of copper(II) from wastewater. J Hazard Mater 345:1–9. https://doi.org/10.1016/j.jhazmat.2017.11.002

Chen W, Zou C, Li X, Liang H (2019) Application of recoverable carbon nanotube nanofluids in solar desalination system: an experimental investigation. Desalination 451:92–101. https://doi.org/10.1016/j.desal.2017.09.025

El-Bialy E, Shalaby SM, Kabeel AE, Fathy AM (2016) Cost analysis for several solar desalination systems. Desalination 384:12–30. https://doi.org/10.1016/j.desal.2016.01.028

Elashmawy M (2020) Experimental study on water extraction from atmospheric air using tubular solar still. J Clean Prod 249:119322. https://doi.org/10.1016/j.jclepro.2019.119322

Essa FA, Abdullah AS, Omara ZM (2020) Rotating discs solar still: new mechanism of desalination. J Clean Prod 275:123200. https://doi.org/10.1016/j.jclepro.2020.123200

Fath HES, Hosny HM (2002) Thermal performance of a single-sloped basin still with an inherent built-in additional condenser. Desalination 142:19–27. https://doi.org/10.1016/S0011-9164(01)00422-2

Gnanaraj SJP, Velmurugan V (2019) An experimental study on the efficacy of modifications in enhancing the performance of single basin double slope solar still. Desalination 467:12–28. https://doi.org/10.1016/j.desal.2019.05.015

Haddad Z, Chaker A, Rahmani A (2017) Improving the basin type solar still performances using a vertical rotating wick. Desalination 418:71–78. https://doi.org/10.1016/j.desal.2017.05.030

Hansen RS, Narayanan CS, Murugavel KK (2015) Performance analysis on inclined solar still with different new wick materials and wire mesh. Desalination 358:1–8. https://doi.org/10.1016/j.desal.2014.12.006

Harish Prashanth KV, Tharanathan RN (2006) Crosslinked chitosan - preparation and characterization. Carbohydr Res 341:169–173. https://doi.org/10.1016/j.carres.2005.10.016

Jamil B, Akhtar N (2017) Effect of specific height on the performance of a single slope solar still: an experimental study. Desalination 414:73–88. https://doi.org/10.1016/j.desal.2017.03.036

Kabeel AE, Hamed AM, El-Agouz SA (2010) Cost analysis of different solar still configurations. Energy 35:2901–2908. https://doi.org/10.1016/j.energy.2010.03.021

Kabeel AE, Khalil A, Omara ZM, Younes MM (2012) Theoretical and experimental parametric study of modified stepped solar still. Desalination 289:12–20. https://doi.org/10.1016/j.desal.2011.12.023

Kabeel AE, Omara ZM, Younes MM (2015) Techniques used to improve the performance of the stepped solar still-a review. Renew Sust Energ Rev 46:178–188. https://doi.org/10.1016/j.rser.2015.02.053

Kabeel AE, Arunkumar T, Denkenberger DC, Sathyamurthy R (2017) Performance enhancement of solar still through efficient heat exchange mechanism – a review. Appl Therm Eng 114:815–836. https://doi.org/10.1016/j.applthermaleng.2016.12.044

Kabeel AE, Sharshir SW, Abdelaziz GB, Halim MA, Swidan A (2019) Improving performance of tubular solar still by controlling the water depth and cover cooling. J Clean Prod 233:848–856. https://doi.org/10.1016/j.jclepro.2019.06.104

Kabeel AE, Sathyamurthy R, Manokar AM, Sharshir SW, Essa FA, Elshiekh AH (2020) Experimental study on tubular solar still using graphene oxide nano particles in phase change material (NPCM's) for fresh water production. J Energy Storage 28:101204. https://doi.org/10.1016/j.est.2020.101204

Khandagre M, Gupta B, Bhalavi J (2019) Design parameters of solar still including application of phase change materials : a review. 4:80–88

Kudret Selçuk M (1964) Design and performance evaluation of a multiple-effect, tilted solar distillation unit. Sol Energy 8:23–30. https://doi.org/10.1016/0038-092X(64)90007-6

Kumar PN, Manokar AM, Madhu B, Kabeel AE, Arunkumar T, Panchal H, Sathyamurthy R (2017) Experimental investigation on the effect of water mass in triangular pyramid solar still integrated to inclined solar still. Groundw Sustain Dev 5:229–234. https://doi.org/10.1016/j.gsd.2017.08.003

Manokar AM, Winston DP, Kabeel AE, Sathyamurthy R (2018) Sustainable fresh water and power production by integrating PV panel in inclined solar still. J Clean Prod 172:2711–2719. https://doi.org/10.1016/j.jclepro.2017.11.140

Modi KV, Modi JG (2019) Performance of single-slope double-basin solar stills with small pile of wick materials. Appl Therm Eng 149: 723–730. https://doi.org/10.1016/j.applthermaleng.2018.12.071

Mohammed AJ (2013) New design of the stepped solar still. J Basrah Res 39:1–8

Nafey AS, Abdelkader M, Abdelmotalip A, Mabrouk AA (2000) Parameters affecting solar still productivity. Energy Convers Manag 41:1797–1809. https://doi.org/10.1016/S0196-8904(99)00188-0

Ni G, Zandavi SH, Javid SM, Boriskina SV, Cooper TA, Chen G (2018) A salt-rejecting floating solar still for low-cost desalination. Energy Environ Sci 11:1510–1519. https://doi.org/10.1039/c8ee00220g

Pal P, Yadav P, Dev R, Singh D (2017) Performance analysis of modified basin type double slope multi–wick solar still. Desalination 422:68–82. https://doi.org/10.1016/j.desal.2017.08.009

Panchal H, Mohan I (2017) Various methods applied to solar still for enhancement of distillate output. Desalination 415:76–89. https://doi.org/10.1016/j.desal.2017.04.015

Panchal H, Sathyamurthy R (2020) Experimental analysis of single-basin solar still with porous fins. Int J Amb Energy 41:563–569. https://doi.org/10.1080/01430750.2017.1360206

Parsa SM, Rahbar A, Javadi YD et al (2020) Energy-matrices, exergy, economic, environmental, exergoeconomic, enviroeconomic, and heat transfer (6E/HT) analysis of two passive/active solar still water desalination nearly 4000m: altitude concept. J Clean Prod 261: 121243. https://doi.org/10.1016/j.jclepro.2020.121243

Patel J, Markam BK, Maiti S (2019) Potable water by solar thermal distillation in solar salt works and performance enhancement by integrating with evacuated tubes. Sol Energy 188:561–572. https://doi.org/10.1016/j.solener.2019.06.026

Prakash P, Velmurugan V (2015) Parameters influencing the productivity of solar stills – a review. Renew Sust Energ Rev 49:585–609. https://doi.org/10.1016/j.rser.2015.04.136

Rabhi K, Nciri R, Nasri F, Ali C, Ben Bacha H (2017) Experimental performance analysis of a modified single-basin single-slope solar still with pin fins absorber and condenser. Desalination 416:86–93. https://doi.org/10.1016/j.desal.2017.04.023

Rahim NHA (2001) Utilisation of new technique to improve the efficiency of horizontal solar desalination still. Desalination 138:121–128. https://doi.org/10.1016/S0011-9164(01)00253-3

Rajaseenivasan T, Srithar K (2017) An investigation into a laboratory scale bubble column humidification dehumidification desalination system powered by biomass energy. Energy Convers Manag 139: 232–244. https://doi.org/10.1016/j.enconman.2017.02.043

Ranjan KR, Kaushik SC (2013) Energy, exergy and thermo-economic analysis of solar distillation systems: a review. Renew Sust Energ Rev 27:709–723. https://doi.org/10.1016/j.rser.2013.07.025

Ritonga H, Nurfadillah A, Rembon FS, Ramadhan LOAN, Nurdin M (2019) Preparation of chitosan-EDTA hydrogel as soil conditioner for soybean plant (Glycine max). Groundw Sustain Dev 9:100277. https://doi.org/10.1016/j.gsd.2019.100277

Sabaa MW, Abdallah HM, Mohamed NA, Mohamed RR (2015) Synthesis, characterization and application of biodegradable crosslinked carboxymethyl chitosan/poly(vinyl alcohol) clay nanocomposites. Mater Sci Eng C 56:363–373. https://doi.org/10.1016/j.msec.2015.06.043

Sathyamurthy R, Kennady HJ, Nagarajan PK, Ahsan A (2014) Factors affecting the performance of triangular pyramid solar still. Desalination 344:383–390. https://doi.org/10.1016/j.desal.2014.04.005

Sathyamurthy R, Kabeel AE, Balasubramanian M, Devarajan M, Sharshir SW, Manokar AM (2020) Experimental study on enhancing the yield from stepped solar still coated using fumed silica nanoparticle in black paint. Mater Lett 272:127873. https://doi.org/10.1016/j.matlet.2020.127873

Shalaby SM, El-Bialy E, El-Sebaii AA (2016) An experimental investigation of a v-corrugated absorber single-basin solar still using PCM. Desalination 398:247–255. https://doi.org/10.1016/j.desal.2016.07.042

Sharshir SW, Ellakany YM, Eltawil MA (2020a) Exergoeconomic and environmental analysis of seawater desalination system augmented with nanoparticles and cotton hung pad. J Clean Prod 248:119180. https://doi.org/10.1016/j.jclepro.2019.119180

Sharshir SW, Peng G, Elsheikh AH, Eltawil MA, Elkadeem MR, Dai H, Zang J, Yang N (2020b) Influence of basin metals and novel wick-metal chips pad on the thermal performance of solar desalination process. J Clean Prod 248:119224. https://doi.org/10.1016/j.jclepro.2019.119224

Shyora A, Patel K, Panchal H (2019) Comparative analysis of stepped and single basin solar still in climate conditions of Gandhinagar Gujarat during winter. Int J Amb Energy 1:1–24. https://doi.org/10.1080/01430750.2019.1612781

Sionkowska A (2006) Effects of solar radiation on collagen and chitosan films. J Photochem Photobiol B Biol 82:9–15. https://doi.org/10.1016/j.jphotobiol.2005.08.003

Sohani A, Hoseinzadeh S, Berenjkar K (2021) Experimental analysis of innovative designs for solar still desalination technologies; an in-depth technical and economic assessment. J Energy Storage 33: 101862. https://doi.org/10.1016/j.est.2020.101862

Srithar K, Rajaseenivasan T, Karthik N, Periyannan M, Gowtham M (2016) Stand alone triple basin solar desalination system with cover cooling and parabolic dish concentrator. Renew Energy 90:157–165. https://doi.org/10.1016/j.renene.2015.12.063

Suneesh PU, Paul J, Jayaprakash R, Kumar S, Denkenberger D (2016) Augmentation of distillate yield in "V"-type inclined wick solar still with cotton gauze cooling under regenerative effect. Cogent Eng 3: 1–10. https://doi.org/10.1080/23311916.2016.1202476

Suresh C, Shanmugan S (2019) Effect of water flow in a solar still using novel materials. J Therm Anal Calorim 5. https://doi.org/10.1007/s10973-019-08449-5

Thalib MM, Manokar AM, Essa FA, Vasimalai N, Sathyamurthy R, Garcia Marquez FP (2020) Comparative study of tubular solar stills with phase change material and nano-enhanced phase change material. Energies:13. https://doi.org/10.3390/en13153989

Wang W, Laumert B (2017) Effect of cavity surface material on the concentrated solar flux distribution for an impinging receiver. Sol Energy Mater Sol Cells 161:177–182. https://doi.org/10.1016/j.solmat.2016.12.008

Xu YX, Kim KM, Hanna MA, Nag D (2005) Chitosan-starch composite film: preparation and characterization. Ind Crop Prod 21:185–192. https://doi.org/10.1016/j.indcrop.2004.03.002

Yousef MS, Hassan H (2020) Energy payback time, exergoeconomic and enviroeconomic analyses of using thermal energy storage system with a solar desalination system: an experimental study. J Clean Prod 270:122082. https://doi.org/10.1016/j.jclepro.2020.122082